Biosensors and Bioelectronics 96 (2017) 201–205

Contents lists available at ScienceDirect

Biosensors and Bioelectronics

journal homepage: www.elsevier.com/locate/bios

Binding-induced DNA walker for signal amplification in highly selective electrochemical detection of protein

Yuhang Ji[1], Lei Zhang[1], Longyi Zhu, Jianping Lei*, Jie Wu, Huangxian Ju

State Key Laboratory of Analytical Chemistry for Life Science, School of Chemistry and Chemical Engineering, Nanjing University, Nanjing 210023, PR China

ARTICLE INFO

Keywords:
Electrochemical detection
DNA walker
Aptasensor
Signal amplification
Protein

ABSTRACT

A binding-induced DNA walker-assisted signal amplification was developed for highly selective electrochemical detection of protein. Firstly, the track of DNA walker was constructed by self-assembly of the high density ferrocene (Fc)-labeled anchor DNA and aptamer 1 on the gold electrode surface. Sequentially, a long swing-arm chain containing aptamer 2 and walking strand DNA was introduced onto gold electrode through aptamers-target specific recognition, and thus initiated walker strand sequences to hybridize with anchor DNA. Then, the DNA walker was activated by the stepwise cleavage of the hybridized anchor DNA by nicking endonuclease to release multiple Fc molecules for signal amplification. Taking thrombin as the model target, the Fc-generated electrochemical signal decreased linearly with logarithm value of thrombin concentration ranging from 10 pM to 100 nM with a detection limit of 2.5 pM under the optimal conditions. By integrating the specific recognition of aptamers to target with the enzymatic cleavage of nicking endonuclease, the aptasensor showed the high selectivity. The binding-induced DNA walker provides a promising strategy for signal amplification in electrochemical biosensor, and has the extensive applications in sensitive and selective detection of the various targets.

1. Introduction

Signal amplification strategies have been widely implanted in electrochemical biosensor to achieve low detection limit and high sensitivity. Generally, there are two types of signal amplification strategies on the basis of nanomaterials (Wu et al., 2014) or biomolecules (Deng et al., 2015). Different from nanomaterial-based strategies, biomolecule-based strategies have excellent biocompatibility in physiological conditions, especially for DNA-based signal amplification tactics such as polymerase chain reaction, rolling circle amplification (Ji et al., 2016), hybridization chain reaction (HCR) (Li et al., 2017; Shuai et al., 2017b), catalytic hairpin assembly (CHA) (Shuai et al., 2016; Zhao et al., 2017) and so on. For example, Li's group designed a two-step signal amplification strategy by combination CHA and HCA for electrochemical detection of DNA with the assistant of external signal molecules and auxiliary probe (Liu et al., 2013). Zhang's group reported a sandwich DNA structure triggered by target DNA, and then initiated HCR reaction to generate electrochemical signal (Yang et al., 2016a). Huang's group developed a series of electrochemical sensing strategies combined nanomaterials with nicking enzyme for signal amplification (Huang et al., 2016; Shuai et al., 2017a). Although the biomolecule-based amplifications have been achieved for electrochemical analysis, these strategies still suffer from some limitations, such as slow electron transfer of amplified DNA structures and low turnover of catalytic cycle. Recent emergence of DNA walker strategy might provide new approach to solve the problem.

DNA walker as a type of molecular machine has been demonstrated to manipulate specific DNA (walking strand) to move autonomously along programmed oligonucleotide tracks such as double stranded DNA (Liu et al., 2016), DNA origami (Zhou et al., 2015), and DNA monolayer (Qu et al., 2017; Yehl et al., 2016). Usually, DNA walkers are propelled by DNAzymes (Pan et al., 2015), protein enzymes (Awaja et al., 2015) and strand displacement (Jung et al., 2016). The movements of walker can destruct the tracks and generate single-stranded product for signal amplification, which can be used as transducer in analytical and diagnostic applications (Peng et al., 2017; Li et al., 2015). In fact, a series of DNA walkers were constructed along a three-dimensional DNA-Au nanoparticle track and cleaved DNA substrates with a nicking endonuclease to release payloads for fluorescence assays (Yang et al., 2016b; Zhang et al., 2015). A free-running DNA walker was also proposed as electrochemical aptasensor formed by DNA self-assembly to detect breast cancer cell via chronocoulometry measure-

* Corresponding author.
E-mail address: jpl@nju.edu.cn (J. Lei).
[1] These authors contributed equally to this work.

http://dx.doi.org/10.1016/j.bios.2017.05.008
Received 14 April 2017; Received in revised form 2 May 2017; Accepted 4 May 2017
Available online 04 May 2017

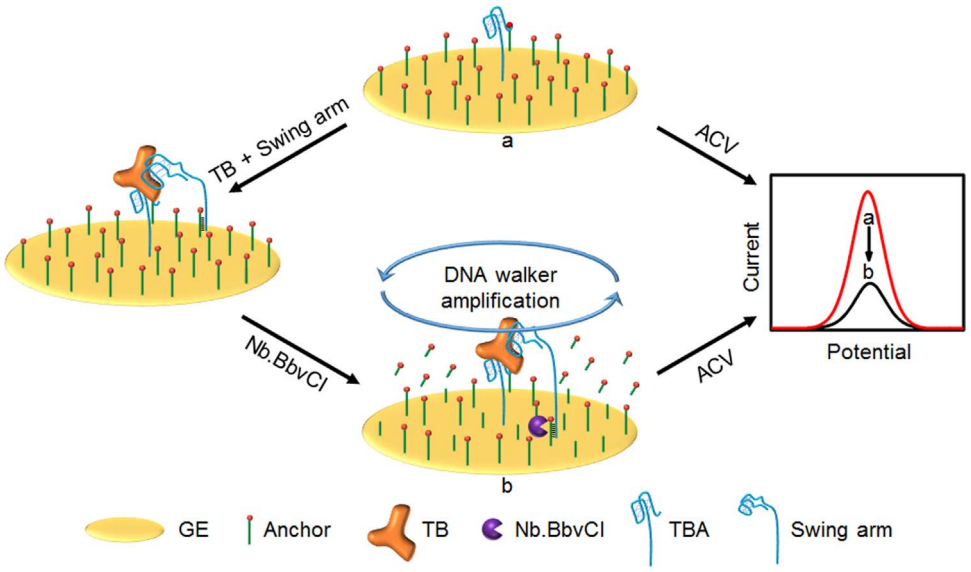

Fig. 1. Schematic illustration of design and analytical procedure of binding-induced DNA walker-assisted signal amplification for electrochemical detection of protein.

ment (Cai et al., 2016). Distinct from the DNA self-assembled walker, a binding-induced DNA walker harnesses specific target binding to trigger assembly of separate DNA components for movement. Therefore, the binding-induced DNA walkers initiate hundreds of signal molecules in response to a single binding event with high specificity, providing a promising tool to design signal amplification method.

In this work, a binding-induced DNA walker is for the first time proposed in the electrochemical aptasensor on the gold electrode (GE). Firstly, the aptasensor was constructed by self-assembly of ferrocene (Fc) labeled anchor as both DNA walker's track and signal molecule on GE with a certain number of thrombin aptamer 1 (TBA) (Fig. 1). Meanwhile, a swing arm DNA was designed consisting of a thrombin aptamer 2 (HD22) and walking strand with repeated T bases as the spacer. Due to only 7 complementary nucleotides between swing arm and anchor so that their hybrid is unstable at ambient temperature. When adding thrombin (TB) and swing arm DNA on the aptasensor, a sandwich structure was formed through the binding of thrombin with the two aptamers, which places the swing arm onto the GE surface. Therefore, the complementary sequences of swing arm and anchor are brought into close proximity, allowing for intramolecular binding-induced assembly to form the duplex. Then nicking endonuclease Nb. BbvCI can specifically cut the hybridized anchor, resulting in releasing Fc molecule from electrode surface to solution and liberate walking strand as free end again. Subsequently, the free walking strand would bind with another anchor to repeat the Nb.BbvCI nicking across the successive interface of electrode to release multiple Fc molecules for signal amplification. Therefore, a highly sensitive and selective strategy was achieved for the detection of target protein. The proposed binding-induced DNA walker provides a promising tool to construct efficient and rapid electrochemical detection strategy for a variety of biomarkers.

2. Experimental

2.1. Chemicals

Nb. BbvCI and CutSmart Buffer (50 mM potassium acetate, 20 mM Tris-acetate, 10 mM magnesium acetate, 100 μg mL^{-1} BSA) were obtained from New England Biolabs Inc. (USA). Thrombin, hemoglobin (Hb), bovine serum albumin (BSA), L-cysteine (L-cys), 6-mercapto-1-hexanol (MCH), hexaammineruthenium(III) chloride (RuHex, 98%), ethylene diamine tetraacetic acid (EDTA) and tris(2-carboxyethyl) phosphine hydrochloride (TCEP) were purchased from Sigma-Aldrich Inc. (USA). TE buffer (10 mM Tris-HCl, 1 mM EDTA, 1 M NaCl, pH 7.4) and Tris-HCl buffer (20 mM, 140 mM NaCl, 5 mM KCl, 1 mM $CaCl_2$, 1 mM $MgCl_2$, pH 7.4) were prepared in this work.

Oligonucleotides were synthesized by Sangon Biotechnology Co. Ltd. (Shanghai, China). The sequences of these oligonucleotides were as follows from 5′ end to 3′ end:

Anchor: HS-TTTTTTTTTTTGTCGTGCTGAGGTT-Fc
Control anchor: HS-TTTTTTTTTTTGTCGTGCTGAGGTT
TBA: HS-$(T)_{25}$**GGTTGGTGTGGTTGG**
Blocker: GAGGACACG
Swing arms (n=2, 12, 22, 32, 42, 52):

AGTCCGTGGTAGGGCAGGTTGGGGTGACT$(T)_n$GTCGTGT*CCTCAGC*

The italic and bold bases represent walking strand and thrombin aptamers, respectively.

2.2. Preparation of aptasensor

Before modification, GE was cleaned by exposing into piranha solution (H_2SO_4/H_2O_2, 3:1) for 10 min, polished with 0.05 μm α-Al_2O_3 slurry, and electrochemically cleaned in 1 M H_2SO_4 by potential scanning between −0.2 and +1.6 V at a scan rate of 4 V s^{-1} for 40 scans until a reproducible cyclic voltammogram (CV) signal was obtained. 50 μL of anchor (2.0 μM) and 2.5 μL of TBA (2.0 μM) were incubated with 5.0 μL of TCEP (10 mM) for 1 h to allow reduction of disulfide bonds and finally diluted to a total volume of 100 μL to obtain a mixture of 1.0 μM anchor and 0.05 μM TBA. 5 μL of the above solution was dropped on GE and incubated at 37 °C for 2 h. After rinsing with phosphate buffer (PBS) and drying with nitrogen, 5 μL of 1 mM MCH was dropped on the electrode for 1 h at 37 °C to block the unmodified sites. Finally, the electrochemical DNA aptasensor was washed with PBS thoroughly to remove unfixed MCH and DNA.

2.3. Measurement procedure

The electrochemical measurements were automatically performed on a CHI 660D electrochemical workstation (Shanghai CH Instrument, China) with a conventional three-electrode system composed of a platinum wire as counter, saturated calomel electrode as reference

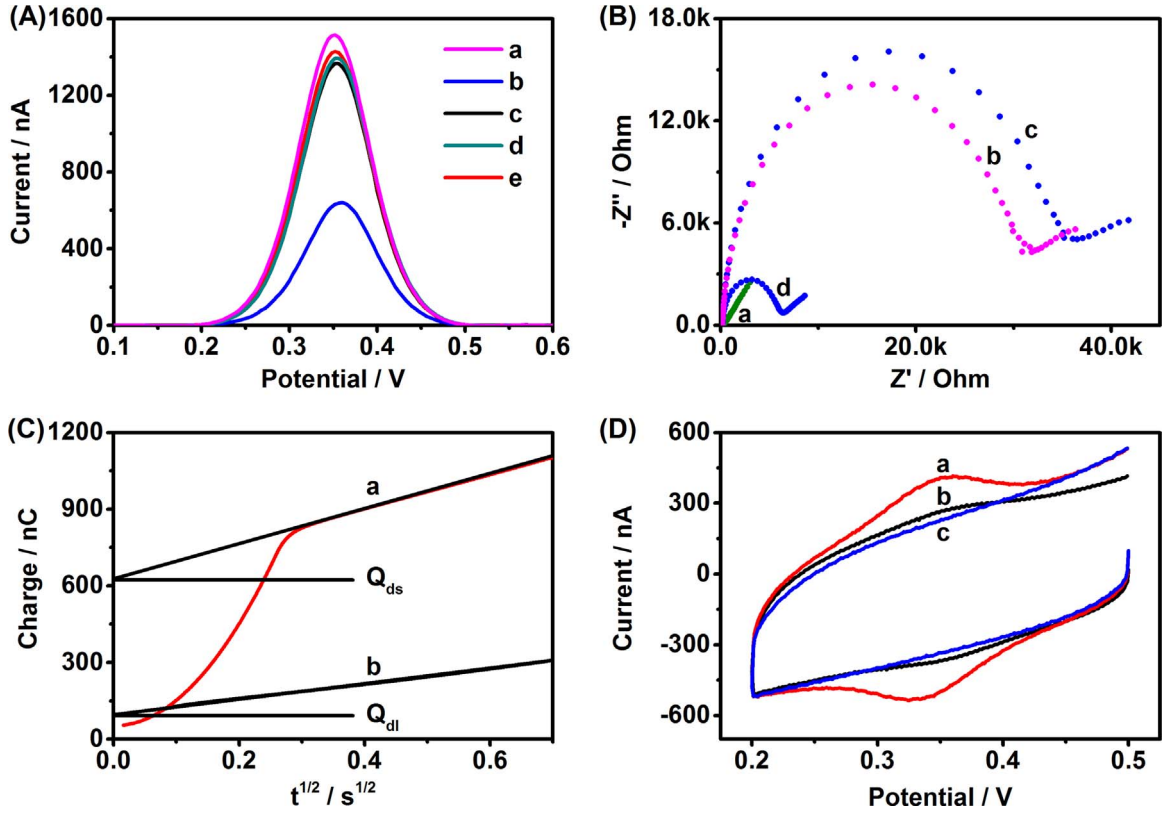

Fig. 2. (A) ACV response of the aptasensor after 2-h incubation with (a) ultrapure water, (b) 100 nM swing arm, 10 nM TB and 1 U Nb.BbvCI. (c), (d) and (e) are (b) in the absence of Nb.BbvCI, swing arm and TB, respectively. (B) EIS of (a) bare GE, (b) the aptasensor, (c) the aptasensor after incubation with TB and swing arm, and (d), (c) + Nb.BbvCI. (C) CC curves for (a) the aptasensor and (b) MCH modified GE in PBS containing 50 μM RuHex. The CC intercept ($t^{1/2}$ =0) represents the charges of RuHex confined at the electrode surface. Q_{dl} and Q_{ds} are the capacitive charge and the total charge containing the capacitive charge and the adsorbed reactant charge, respectively. (D) CV curves for (a) the aptasensor, (b) the aptasensor after incubation with 100 nM swing arm, 10 nM TB and 1 U Nb.BbvCI, and (c) control anchor, MCH and TBA modified GE in pH 7.4 PBS.

and the 2-mm diameter GE as working electrodes. Prior to measurement, a mixed solution was prepared, which contained 100 nM swing arm, 200 nM blocker and various concentrations of thrombin in Tris-HCl buffer. Then, 5.0 μL of the mixture was dropped on the aptasensor surface and incubated at room temperature for 30 min. Sequentially, 5.0 μL of Nb.BbvCI (0.2 U μL^{-1}) in 1× CutSmart Buffer was added and incubated at 37 °C for 2 h. After washed with Tris-HCl buffer, the biosensor was immersed in 10 mM PBS containing 0.1 M $NaClO_4$ for alternating current voltammetry (ACV) detection from +0.1 to +0.6 V with a step potential of 4 mV, a frequency of 25 Hz and an amplitude of 25 mV.

3. Results and discussion

3.1. Feasibility of binding-induced DNA walker aptasensor

The feasibility of this aptasensor was executed in different solutions using ACV (Fig. 2A). Firstly, an obvious oxidation peak of Fc at +0.36 V (curve a) indicated the successful modification of anchor onto GE. After incubating with TB and swing arm, a slight decrease was observed due to the formation of TBA-thrombin-swing arm (TTS) sandwich structure (curve c). After adding Nb.BbvCI, a greatly decreased Fc signal was observed (curve b), which is attributed to the stepwise cutting of anchor once the formation of double-stranded DNA between anchor and the walking strand sequence of swing arm. As control, in the absence of swing arm (curve d) or target thrombin (curve e), none of which was observed the signal change. These results indicated that the DNA walker was triggered by the specific binding of thrombin with two aptamers, and led to the amplified Fc-generated signal for electrochemical detection.

Electrochemical impedance spectroscopic (EIS) measurements were employed to characterize the preparation of aptasensor (Fig. 2B). The bare GE showed a relatively small electron transfer resistance (R_{et}) (curve a). After immobilization of anchor and TBA, R_{et} obviously increased (curve b), which was attributed to that the negatively charged DNA sentence repelled the $[Fe(CN)_6]^{3+/4+}$ to the electrode surface, indicating the successful immobilization of anchor and TBA on GE surface. In the presence of TB and swing arm, the formed TTS sandwich structure blocked the electron transfer and therefore led to an enhanced R_{et} (curve c). However, the R_{et} of the aptasensor was significantly reduced after the cleavage of multiple anchors by Nb.BbvCI (curve d).

Chronocoulometry (CC) measurements were conducted to estimate DNA density on the GE by using a cationic redox marker (RuHex). According to Cottrell expression and Faraday's law (Yang et al., 2016a; Yao et al., 2014), the density of anchor DNA was estimated to be approximately 1.3×10^{13} molecules per cm^2 (Fig. 2C). Thus, the average area each anchor occupies on GE was 7.5 nm^2, and the distance between two adjacent anchors was calculated to be 2.7 nm. Assuming DNA as single-straight strand, the length of TTS sandwich structure was estimated 38.3 nm and thus the area of TTS was 4600 nm^2. Therefore, approximate 610 anchors calculated by dividing the TTS area by single anchor area, could be reached by one swing arm, indicating the feasibility of DNA walker-involved signal amplification strategy.

The DNA walker-regulated recycling amplification reaction was also demonstrated by CV. Fig. 2D displays CV curves of the total amount of Fc immobilized on GE before (curve a) and after (curve b) adding TB, swing arm and Nb.BbvCI, which can be calculated from the area under either the anodic or the cathodic peak corrected from the background current (curve c) (Anne et al., 2003). The proportion of anchor cut by Nb.BbvCI was calculated to be approximate 70%, the result of which

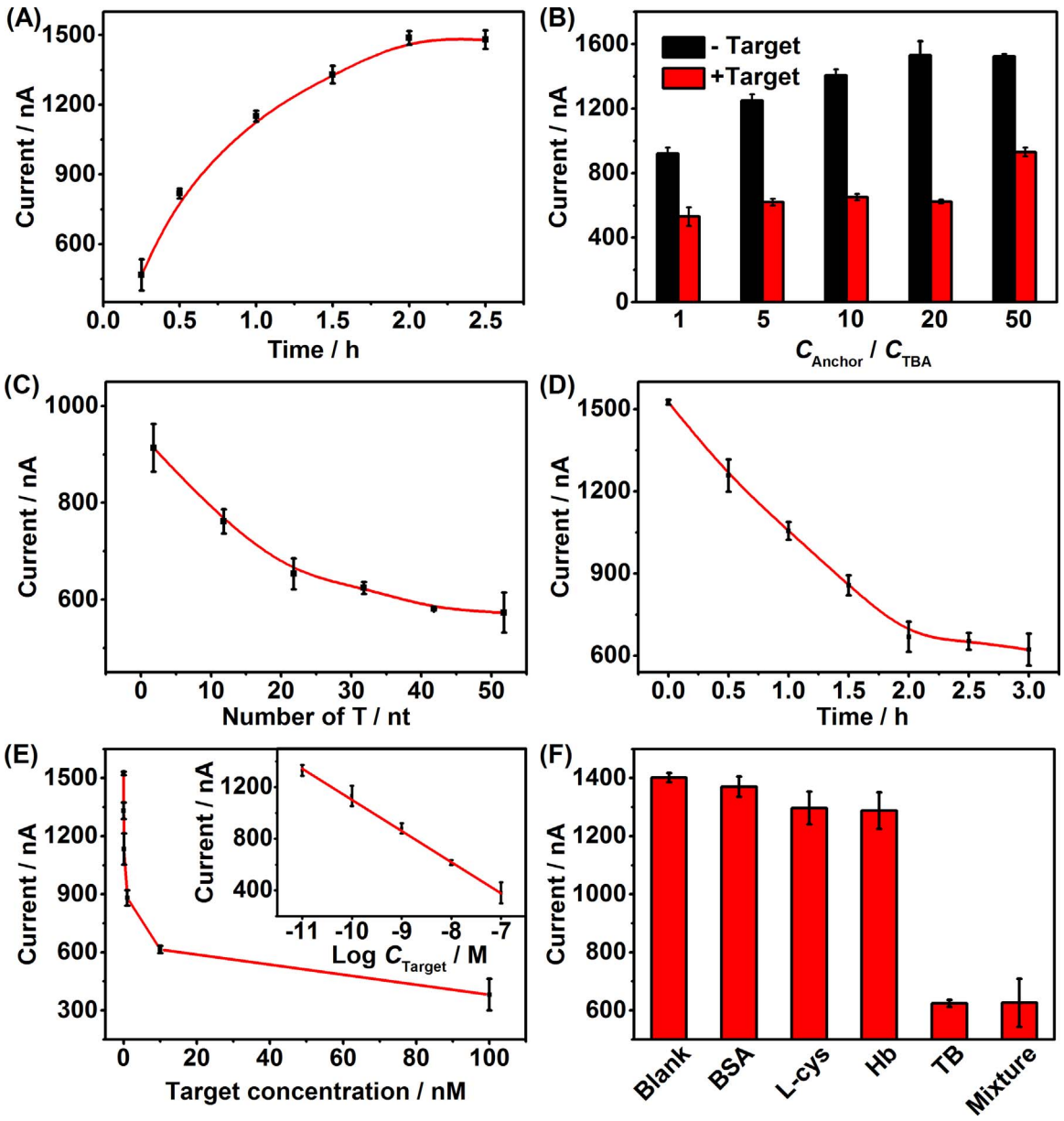

Fig. 3. Effects of (A) immobilization time and (B) the concentration ratio of anchor DNA to TBA for self-assembly of aptasensor, (C) number of T bases as spacer sequence between aptamer 2 and walking strand DNA in the swing arm, and (D) Nb.BbvCI nicking time on the ACV response. (E) The ACV response of the aptasensor to TB at different concentrations. Inset is the linear relationship between the peak current and logarithm of target concentration. (F) Specificity of the aptasensor against 100 nM BSA or L-cys or Hb, and response to 10 nM TB or the mixture of 10 nM TB, 100 nM BSA, L-cys and Hb.

was in agreement with ACV.

3.2. Optimization of experimental parameters

The density of DNA immobilized on the gold electrode was important to the analytical performance of the biosensor, especially affected the mechanical property of DNA walker. Using TE buffer as the optimized reaction buffer, the maximal signal was achieved after incubating with anchor solution for 2 h at 37 °C (Fig. 3A). The ratio of anchor to TBA immobilized on the GE surface is another important parameter that influences the electrochemical signal. As shown in Fig. 3B, the increase of TBA concentration resulted in the decreased electrochemical signal due to the competitive effect between TBA and Fc-modified anchor during the self-assembly of DNA monolayer. However, low TBA concentration had a significant effect on the sensitivity of target recognition. Overall, the anchors with 20-fold concentration more than TBA were selected as self-assembled DNA walker track.

Considering that the flexibility of the whole swing arm strand is significant for both target recognition and walker DNA hybridization on GE surface. The number of thymine (T) DNA nucleotides as the spacer sequences were investigated. As shown in Fig. 3C, 32-nt T was chosen as the space sequence in swing arm for the optimal signal readout. Additionally, enzymatic cleavage time of Nb.BbvCI was optimized. After the Nb.BbvCI was added on the aptasensor, ACV signal decreased with the increase of enzymatic reaction time and reached a platform with the value of 600 nA. Therefore, 2 h was chosen as the optimal cleavage reaction time (Fig. 3D).

3.3. Assay performance

To assess the analytical performance of the proposed aptasensor, standard solutions of TB at different concentrations were incubated with the proposed aptasensor in the optimized experimental conditions

(Fig. 3E), which showed the decreasing ACV signal at +0.36 V with the increasing target concentrations. The calibration plot showed a linear relationship between the peak current and the logarithm value of TB concentration ranging from 0.01 to 100 nM with a correlation coefficient of 0.9974 (Fig. 3E). The detection limit at a signal-to-noise ratio of 3 was calculated to be 2.5 pM, which was much lower than 0.07 nM of graphene oxide modified pencil graphite electrode (Ahour and Ahsani, 2016), 3 nM of electrochemical aptasensor based on switching structure of aptamer from DNA/DNA duplex to DNA/target complex (Yan et al., 2011), and 1.8 nM of triple-helix aptamer-based fluorescent assay (Xu et al., 2015). When the biosensor was stored at −20 °C for 7 days, it retained 94.0% of its initial current response, indicating acceptable stability. In addition, the good reproducibility of this aptasensor was manifested via executing a series of five duplicate measurements of 1.0 nM TB with a relative standard deviation of 3.5%.

To evaluate the specificity of the developed aptasensor, 10-fold interfering substances, including BSA, Hb and L-cys were tested (Fig. 3F). No significant change in the electrochemical response was observed when the aptasensor was incubated with these substances, because the TTS structure could not be formed in presence of aptamer-interfering protein. However, the electrochemical response substantially decreased upon the incubation of TB (10 nM) or mixture of TB and the interferents, which was attributed to the high specificity of aptamer to the target, showing the practicability of the aptasensor in complex samples.

4. Conclusion

In this work, the binding-induced DNA walker is successfully introduced in electrochemical aptasensor for thrombin detection. The DNA walker was activated by forming a sandwich structure of TBA-TB-swing arm on the surface of GE in the confined area. Theoretically, approximate 610 anchors could be reached by walking chain on one swing arm, leading to the significant signal amplification. Under optimal conditions, the proposed assay showed a thrombin detection range over 4 orders of magnitude with a detection limit of pM level. By coupling with the specific cleavage of nicking endonuclease, the binding-induced DNA walker demonstrated the high sensitivity against the interfering substances. The binding-induced DNA walker provides a promising tool for signal transduction in bioassay and clinical diagnosis.

Acknowledgements

We gratefully acknowledge the National Natural Science Foundation of China (21375060, 21635005, 21605082, 21675084) and Program for New Century Excellent Talents in University of Ministry of Education of China (NCET-13-0283).

References

Ahour, F., Ahsani, M.K., 2016. Biosens. Bioelectron. 86, 764–769.
Anne, A., Bouchardon, A., Moiroux, J., 2003. J. Am. Chem. Soc. 125, 1112–1113.
Awaja, F., Wakelin, E.A., Sage, J., Altaee, A., 2015. Prog. Mater. Sci. 74, 308–331.
Cai, S.X., Chen, M., Liu, M.M., He, W.H., Liu, Z.J., Wu, D.Z., Xia, Y.K., Yang, H.H., Chen, J.H., 2016. Biosens. Bioelectron. 85, 184–189.
Deng, H.M., Gao, Z.Q., 2015. Anal. Chim. Acta 853, 30–45.
Huang, K.J., Shuai, H.J., Zhang, J.Z., 2016. Biosens. Bioelectron. 77, 66–75.
Ji, J.J., Liu, Y.J., Wei, W., Zhang, Y.J., Liu, S.Q., 2016. Biosens. Bioelectron. 85, 25–31.
Jung, C., Allen, P.B., Ellington, A.D., 2016. Nat. Nanotechnol. 11, 157–163.
Li, C., Li, X.X., Wei, L.M., Liu, M.Y., Chen, Y.Y., Li, G.X., 2015. Chem. Sci. 6, 4311–4317.
Li, X., Xu, X.W., Song, J., Xue, Q.W., Li, C.Z., Jiang, W., 2017. Biosens. Bioelectron. 91, 631–636.
Liu, M.H., Cheng, J., Tee, S.R., Streelatha, S., Loh, L.Y., Wang, Z.S., 2016. ACS Nano 10, 5882–5890.
Liu, S.F., Wang, Y., Ming, J.J., Lin, Y., Cheng, C.B., Li, F., 2013. Biosens. Bioelectron. 49, 472–477.
Pan, J., Li, F.R., Chen, H.R., Choi, J.H., 2015. Curr. Opin. Biotechnol. 34, 56–64.
Peng, H.Y., Li, X.F., Zhang, H.Q., Le, X.C., 2017. Nat. Commun. 8, 14378.
Qu, X.M., Zhu, D., Yao, G.B., Su, S., Chao, J., Liu, H.J., Zuo, X.L., Wang, L.H., Shi, J.Y., Wang, L.H., Huang, W., Pei, H., Fan, C.H., 2017. Angew. Chem. Int. Ed. 56, 1855–1858.
Shuai, H.L., Huang, K.J., Xing, L.L., Chen, Y.X., 2016. Biosens. Bioelectron. 86, 337–345.
Shuai, H.L., Huang, K.J., Chen, Y.X., Fang, L.X., Jia, M.P., 2017a. Biosens. Bioelectron. 89, 989–997.
Shuai, H.L., Wu, X., Huang, K.J., Zhai, Z.B., 2017b. Biosens. Bioelectron. 94, 616–625.
Wu, L., Xiong, E.H., Zhang, X., Zhang, X.H., Chen, J.H., 2014. Nano Today 9, 197–211.
Xu, N., Wang, Q.B., Lei, J.P., Liu, L., Ju, H.X., 2015. Talanta 132, 387–391.
Yan, F.F., Wang, F., Chen, Z.L., 2011. Sens. Actuators B 160, 1380–1385.
Yang, H., Gao, Y., Wang, S.Q., Qin, Y., Xu, L., Jin, D., Yang, D., Zhang, G.J., 2016a. Biosens. Bioelectron. 80, 450–455.
Yang, X.L., Tang, Y.N., Mason, S.D., Chen, J.B., Li, F., 2016b. ACS Nano 10, 2324–2330.
Yao, B., Liu, Y.C., Tabata, M., Zhu, H.T.Z., Miyahara, Y., 2014. Chem. Commun. 50, 9704–9706.
Yehl, K., Mugler, A., Vivek, S., Liu, Y., Zhang, Y., Fan, M.Z., Weeks, E.R., Salaita, K., 2016. Nat. Nanotechnol. 11, 184–190.
Zhang, H.Q., Lai, M.D., Zuehlke, A., Peng, H.Y., Li, X.F., Le, X.C., 2015. Angew. Chem. Int. Ed. 54, 14326–14330.
Zhao, J.M., Jing, P., Xue, S.Y., Xu, W.J., 2017. Biosens. Bioelectron. 87, 157–163.
Zhou, C., Duan, X.Y., Liu, N., 2015. Nat. Commun. 6, 8102.